

Theory of local electronic properties and finite-size effects in nanoscale open chains

Andre M. C. Souza^{1,2} and Hans Herrmann^{3,4}

¹*Institut für Computerphysik, Universität Stuttgart, Pfaffenwaldring 27, 70569 Stuttgart, Germany*

²*Departamento de Física, Universidade Federal de Sergipe, 49100-000 Sao Cristovao-SE, Brazil*

³*Computational Physics, IfB, ETH Hönggerberg, HIF E 12, CH-8093 Zürich, Switzerland*

⁴*Departamento de Física, Universidade Federal do Ceará, 60451-970 Fortaleza-CE, Brazil*

(Received 10 September 2007; revised manuscript received 14 January 2008; published 13 February 2008)

The local electronic structure of nanoscale chains is investigated theoretically. We propose a mechanism to explain the even-odd oscillation observed in the length distribution of atom chains. We study the spatial peak structure as obtained by scanning-tunneling-microscopy constant-current topography as a function of the electron-electron interaction, band filling, and temperature. The site-dependent magnetic moment is also examined.

DOI: [10.1103/PhysRevB.77.085416](https://doi.org/10.1103/PhysRevB.77.085416)

PACS number(s): 71.10.Fd, 71.10.Pm, 73.22.-f, 75.75.+a

I. INTRODUCTION

The recent advances in the manufacturing of structures on the nanoscale, with dimensions that are intermediate in size between isolated atoms and molecules and bulk materials, has opened up numerous possibilities for constructing new devices. In particular, recently the effects of electronic quantum confinement within chains of finite length have been studied.¹⁻⁶ With the help of scanning tunneling microscopy (STM) the formation of quantized localized states in the pseudogap of the substrate bulk band in chains at semiconductor or insulator surfaces has been observed.¹

The investigation of the electronic properties of nanoscale atomic clusters is particularly interesting since they suffer strong effects due to the finite chain length. The breaking of translational symmetry creates electronic end states. The electronic quantum confinement on chains of finite length changes the density of states. The conductivity along the chain shows spatial variations.¹⁻³ Direct observation of the local electronic structure on a nanoscale atomic chain by STM stresses the importance of exploring these effects theoretically.

While some STM measurements can be explained on the basis of noninteracting electrons,¹⁻³ others instead suggest a strong interaction between electrons,⁶ indicating the possibility of a description using the Hubbard model. Results for extremely small systems without a systematic extrapolation to larger systems would not have been appropriate some years ago, when nanoscale devices were only known as a theoretical possibility. To manipulate nanostructures, it has become important, not only to obtain new insights regarding theoretical models, but certainly also to better understand the physical properties of these systems.

In this paper we study theoretically the local behavior of the physical quantities of open chains on the nanoscale. We report on site-dependent properties of the electronic quantum confinement within finite-length chains. This theory allows for an interpretation of experimental results. We studied two different aspects of these systems. First, considering only the electronic structure, we introduce a model that captures qualitatively the experimental chain length distribution. For this case, we analyzed the internal structure of atom chains

through the site-dependent occupation number along the axis of the chain for one electron. Second, we studied the electron-electron interaction by using the Hubbard model to understand the main effects of electronic quantum confinement within finite-length chains.

The organization of this paper is as follows. Our investigation of the chain length distribution using the tight-binding approach is presented in Sec. II. The results for local occupation numbers and for the site-dependent magnetic moment as a function of the electron-electron interaction, band filling, and temperature on electronic quantum confinement within finite-length chains are presented in Sec. III. Our conclusions are presented in Sec. IV.

II. TIGHT-BINDING APPROACH

A. Introduction

The fitting of experimental wave vectors of nanoscale atomic clusters has shown a one-dimensional (1D) free electron band dispersion relation.^{1,7} The 1D quantum potential well has been proposed to describe the confinement of the electrons and the local conductivity determined by the superposition of wave functions.^{1,2,8} Here, the experimental results are described by the site-dependent occupation number along the chain. We have used the tight-binding Hamiltonian

$$\mathcal{H}_0 = -t \sum_{i\alpha} (c_{i\alpha}^\dagger c_{i+1\alpha} + \text{H.c.}), \quad (1)$$

where $c_{i\alpha}^\dagger$ ($c_{i\alpha}$) is the creation (annihilation) operator for electrons of spin α at site i and t is the nearest-neighbor hopping integral representing the overlap of electron wave functions. To gain a quantitative picture of the on-site dependence on a chain of N atoms, we have computed the local occupation number

$$n_m(i) = \langle \Psi_m | \hat{n}_i | \Psi_m \rangle / N, \quad (2)$$

where $\hat{n}_i = \hat{n}_{i\uparrow} + \hat{n}_{i\downarrow}$, $\hat{n}_{i\alpha} = c_{i\alpha}^\dagger c_{i\alpha}$, and $|\Psi_m\rangle$ is the m th eigenvector with energy E_m .

We analyze the experimental data of the eigenenergies for chains of 3, 5, 7, 9, and 15 atoms extracted from Ref. 1. We have fitted the data taking the experimental ground-state en-

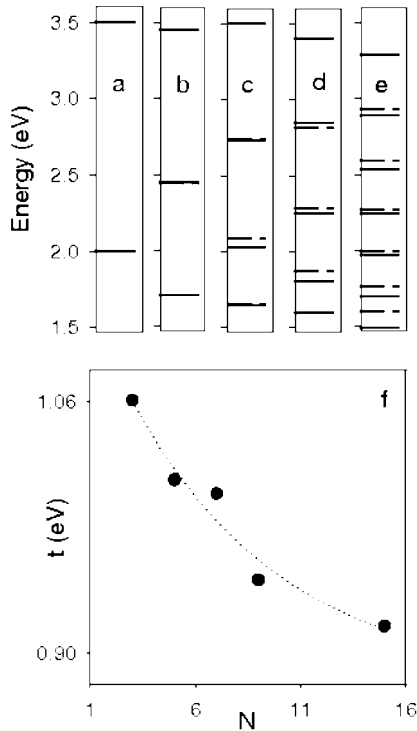


FIG. 1. Experimental (solid line), extracted from Ref. 1, and theoretical (dotted line) eigenenergies for chains of (a) 3, (b) 5, (c) 7, (d) 9, and (e) 15 atoms. (f) The electron hopping strength t as a function of the chain length.

ergies and considering t , in the tight-binding Hamiltonian of Eq. (1), conveniently to obtain the experimental bandwidths. The theoretical and experimental energy spectra are shown in Figs. 1(a)–1(e). The experimental data are reproduced. The electron hopping strength as a function of chain length can be observed in Fig. 1(f). Note that, as the chain length increases, the hopping strength decreases.

In the following will investigate the length distribution of atom chains.

B. Length distribution

Recent results on the distribution of chain segments of gold deposited on a Si surface reveal a relation between the chain length and the cohesive energy.⁹ The size distribution is characterized by a strong peak for a length of one atom and even-odd oscillations, where even chain lengths are favored over odd lengths. To address this problem we propose a simple model. First, we consider the distribution of chain lengths for a completely random distribution of defects to be $\rho(1-\rho)^N$, where ρ is the defect density.⁹ Since chains are fabricated at temperature $T \sim 1000$ °C and considering $t \sim 1$ eV, we must evaluate the canonical average for any quantity x as

$$\langle x \rangle \equiv \sum_i x_i \exp(-E_i/k_B T) / Z, \quad (3)$$

where Z is the partition function. We have obtained a direct relation between the experimental result and the local elec-

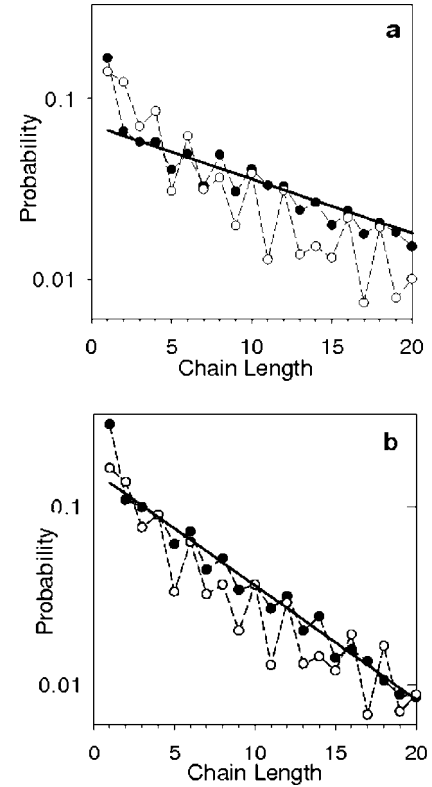


FIG. 2. Experimental (solid circles), extracted from Ref. 9, and theoretical (open circles) distribution of chain lengths for $t/(k_B T) = 0.5$ and (a) low defect density ($\rho=0.0625$) and (b) medium defect density ($\rho=0.125$).

tronic density of the tight-binding model on a finite open chain. We find that on some sites the probability of finding electrons in the excited energy levels is zero. We also observe that these sites correspond to positions that divide the chain in g subchains of equal length. The delocalized electronic structure determines the stability of the atom chain. The cohesive energies are a consequence of the local electronic structure.^{9,10} In particular, we observe that the sites with zero probability to find electrons on odd chains are not binding and result in a larger probability for breaking chains. We assume that there are quantum states breaking a chain of length m into g pieces of length N . It follows that $g \equiv g_{m,N} = (m+1)/(N+1)$, and we can write the distribution of chain lengths as

$$P(N) = A \sum_{m=1}^{\infty} \rho(1-\rho)^m \langle q(m,N) \rangle, \quad (4)$$

where A is a normalization constant, $q_i(m,N) = g_{k,N} \delta_{kN}$, $k = k(m,i)$ is a nontrivial function obtained numerically, and δ_{kN} is Kronecker's delta.

Figure 2 shows the experimental data, extracted from Ref. 9, and our theoretical chain length distribution for low and medium defect densities. The even-odd oscillations are clearly visible. Notably, the present model captures qualitatively the experimental chain length distribution, considering only the electronic structure effects. The quantitative dis-

agreement between theory and experiment is due to the coupling of the electronic structure with the substrate. This coupling was observed in Ref. 9 using photoemission measurements of the electronic scattering vectors at the Fermi surface of the surface states.

Furthermore, the change in chain length obtained by comparing STM images of the same sample region taken at different voltage⁷ is also confirmed by our results. Taking different voltages in STM, the system can fall into an energy level that singles out a position which divides the chain into subchains. An additional nearest-neighbor interaction, reflecting the end states in the chains, was used to describe this effect in Ref. 7 and has already been observed in other STM topography data.^{11,12}

III. ELECTRON-ELECTRON INTERACTION

In addition to the tight-binding model, containing one electron, it is possible to vary the band filling of chain structures.¹ A strong electronic interaction was found for small chains of Mn on CuN, and the STM data were consistent with the Heisenberg model results.⁶ In this case, the effect of electron-electron interaction is particularly important.

The possibility of explaining some STM measurements by the tight-binding model¹⁻³ and others measurements by the Heisenberg model⁶ indicates that we can use the Hubbard model. The 1D Hubbard model is defined by the Hamiltonian

$$\mathcal{H} = \mathcal{H}_0 + U \sum_i \hat{n}_{i\uparrow} \hat{n}_{i\downarrow}, \quad (5)$$

where U is the on-site Coulomb (electron-electron) interaction.

Some solutions of the 1D Hubbard model have been known since the 1960s.¹³ The local behavior of the physical quantities is, however, not completely known. Only partial information is available.¹⁴⁻¹⁶ For example, the spatial dependence of the occupation number and of the magnetization was calculated for the 1D Hubbard model with open boundary conditions combining numerical computations from density-matrix renormalization group and Bethe-ansatz methods.¹⁷ Friedel oscillations for the density and the magnetization in open Hubbard chains have been obtained previously (see Ref. 18 and references therein); however, the focus of these studies has been to analyze macroscopic properties.

We perform exact calculations of 1D systems having N atoms described by the Hubbard model. We use the standard direct diagonalization method^{19,20} and impose open boundary conditions in order to break the translational symmetry. This approach is very well suited for small-sized clusters as studied here; however, it is very inefficient if we increase the size of the system. Monte Carlo methods have proven efficient in studying systems with a large number of atoms, and thus a modern quantum Monte Carlo method²¹ is probably the more efficient approach to study temperature-dependent local quantities with the 1D Hubbard model with open boundary conditions.

We have found in a half-filled band for $U=0$ that the

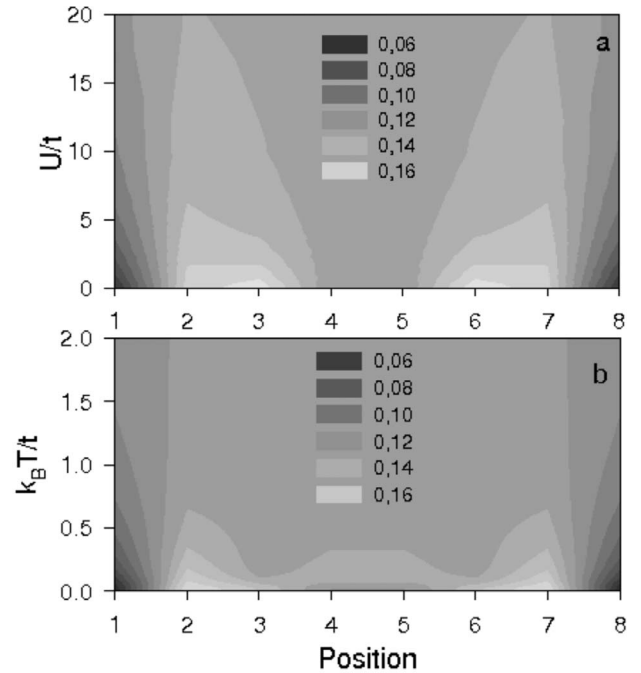


FIG. 3. Values of $n_0(i)$ for a chain of eight sites in the quarter-filled band (a) versus U/t for temperature $T=0$ and (b) versus T for $U/t=8$.

occupation number of the ground state is site *independent*. For $U>0$ this result is valid for all states. This is relevant in order to evaluate the thermodynamic quantity $\langle n(i) \rangle$. We obtain in a half-filled band that $\langle n(i) \rangle = 1/N$ for all sites i , temperatures T , and couplings $U>0$. This is a valuable result because the sites are not equivalent due to the use of open boundary conditions. We observe that, using conformal quantum-field theory, we expect that $\langle n(i) \rangle$ exhibits a Friedel oscillation of an analytical form $\langle n(i) \rangle \approx n/N - \sin(2k_F i)/(2N\pi i^\eta)$,²² which for a half-filled band, $k_F = \pi/2$, and $\langle n(i) \rangle = 1/N$ is site independent.

For other than half-filled bands, we observe a site dependence of $n_m(i)$. For a quarter-filled Hubbard band we have found a rich dependence on U , m , i , and T . Figure 3(a) presents the topography of $n_0(i)$ versus U/t for a chain of eight sites in the quarter-filled band at the temperature $T=0$. For small U/t , the intermediate atoms have larger value than average and the end and central atoms have smaller values. Thus, the probability of finding electrons on the intermediate atoms is higher. The site dependence decreases if the electron-electron interaction increases. For $U/t \rightarrow \infty$ the site dependence disappears, and for all i we find $n_0(i) = 1/8$. We can alternatively fix U/t and vary the temperature in order to cover the other energy states. Figure 3(b) shows this for $U/t=8$ (other values of U/t give similar results). The effect of increasing the temperature is equivalent to an increase of U/t . A large temperature destroys the site dependence of the charges on the chain. While this statement seems true for the local occupation number, there are other quantities, such as intersite spin correlations, that may not follow this rule. In particular, for the half-filled band, $U=0$ is a quantum critical

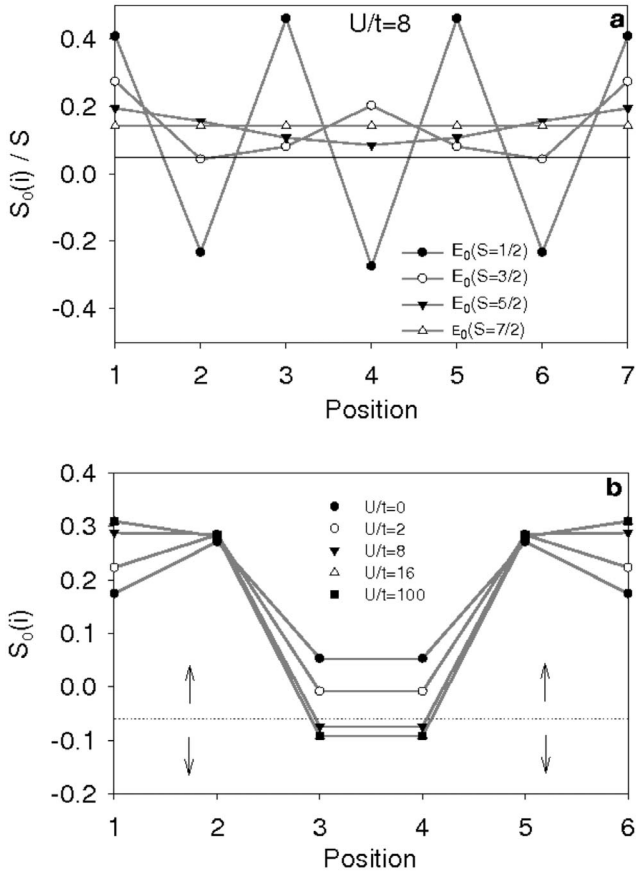


FIG. 4. (a) Site-dependent spin $S_0(i)/S$ versus the position i for a chain of seven sites, for a half-filled band, $U/t=8$, and different total spin $S=\sum_i S_0(i)$. (b) $S_0(i)$ for a chain of six sites for a quarter-filled band versus position i for temperature $T=0$ and $U/t=0, 2, 8, 16$, and 50 .

point and in its vicinity a critical correlation may be characterized by a diverging length.²³ In this case, the correlation at finite temperature²⁴ would be cut off at some finite temperature-dependent thermal coherence length.

For the magnetic properties of finite chains, first-principles calculations have shown that for small chains the spin moment depends on position and cluster length. For example, for Co chains on Pt(111), the spin moments of the end atoms are higher than those of the central atoms and the spin moment of the central atom was found to decrease if the chain size increases.²⁵ Results of the present study are illustrated in Fig. 4. We have studied the local spin number

$$S_m(i) = \langle \Psi_m | \hat{S}_i^z | \Psi_m \rangle, \quad (6)$$

where $\hat{S}_i^z = (\hat{n}_{i\uparrow} - \hat{n}_{i\downarrow})/2$ at site i .

The local spin number $S_0(i)$ versus the position i for a chain of seven sites, for the half-filled band and temperature $T=0$, can be calculated for different total spins $S=\sum_i S_0(i)$ and $U/t=8$. For $S=1/2$ the alternating sign of $S_0(i)$ for odd and even positions gives evidence for an antiferromagnetic structure. The cases $S > 1/2$ have a ferromagnetic structure, since all $S_0(i)$ have the same sign. Site independence is found

for $S=7/2$. On the other hand, when S is between the minimal and maximal values we find a site dependence for $S_0(i)$, with an amplitude that still alternates but not sufficiently to change its sign. For $S=5/2$ we obtain that $S_0(i)$ is larger at the end atoms than at the central atoms as has been found for Co chains on Pt(111).²⁵ We have found that for the case of even total electron number [$n_m = \sum_i n_m(i)$] the $S_m(i)$ is site independent in all m states. $\langle S(i) \rangle = 0$ for all sites i , temperatures T , and couplings U . Considering N even, using the fact that $\langle n(i) \rangle = 1/N$ in the half-filled band and $\langle S(i) \rangle = 0$, the canonical ensemble averages are site independent, like in the mean field, and $\langle n_{\uparrow}(i) \rangle = \langle n_{\downarrow}(i) \rangle = 1/(2N)$, indicating that the open finite even chain is paramagnetic in the half-filled band. It is important to mention that we find site independence although the system has no translational symmetry. The situation for odd finite chains is different. In this case $\langle n(i) \rangle = 1/N$, but $\langle S(i) \rangle$ has a complex site dependence. For the ground state, at $U=0$ we obtain a structure in which $S_0(i) = 1/(N+1)$ and on the nearest-neighbor sites $S_0(i) = 0$. At $U > 0$ we observe an antiferromagnetic structure.

Finally, we explore the dependence of the site-dependent spin on the coupling U . Figure 4(b) shows $S_0(i)$ for the quarter-filled band versus i for a chain of six atoms and typical U/t values. The ground state has $S=1/2$. Here, we show the case $S^z=1/2$. For low U/t all $S_0(i)$ have the same sign favoring a ferromagnetic order and the higher $S_0(i)$ values are at intermediate atoms and the smaller at the central atoms. Increasing U/t the central atoms assume negative values for the spin and the higher $S_0(i)$ shift to the end atoms following a $\uparrow\uparrow\downarrow\downarrow\uparrow\uparrow$ magnetic stripe structure. In fact, for larger chains, the spectral properties of the 1D Hubbard model have been explored in the literature^{26,27} such as the spinon and holon excitations which have provided a precise characterization of the behavior of the local spin for states of nonzero local S^z .

The control and manipulation of the spin rather than the charge of electrons²⁸ in STM could show the very rich behavior of the local magnetic properties presented here. It would be of interest to explore the possibility of obtaining experimental results in the context of magnetic force microscopy (MFM) or STM devices.²⁹ The principle behind the “spin STM” would be the tunneling of electrons between the tip and the surface of the sample generated by a current of spin-polarized electrons. This would generate images that are sensitive to the spin polarization of the electrons. The site-dependent magnetic moment (spin) shown here could be confirmed by these experiments.

IV. CONCLUSION

We have shown that the spatial peak structure of STM constant-current topography can be explained in terms of the site-dependent occupation number. We interpret the even-odd oscillation of the length distribution of atom chains. We also have studied the spatial structure of the electronic charge and spin on finite chains, involving band filling, temperature, and electron-electron interaction, and we examined the site-dependent magnetic moment (spin) indicating properties that

may be confirmed by a possible STM device sensitive to the spin polarization of the electrons. This work provides a simple theoretical explanation for the electronic confinement in atomic chains and opens up a way for a more detailed analysis of the recent STM measurements.

ACKNOWLEDGMENTS

The help of E. Parteli is gratefully acknowledged. This work was supported by CNPq (Brazil) and DAAD (Germany).

-
- ¹S. Folsch, P. Hyldgaard, R. Koch, and K. H. Ploog, *Phys. Rev. Lett.* **92**, 056803 (2004).
²N. Nilius, T. M. Wallis, and W. Ho, *Science* **297**, 1853 (2002).
³F. J. Himpsel, J. L. McChesney, J. N. Crain, A. Kirakosian, V. Perez-Dieste, N. L. Abbott, Y. Y. Luk, P. F. Nealey, and D. Y. Petrovykh, *J. Phys. Chem. B* **108**, 14484 (2004).
⁴V. Vescoli, F. Zwick, W. Henderson, L. Degiorgi, M. Grioni, G. Gruner, and L. K. Montgomery, *Eur. Phys. J. B* **13**, 503 (2000).
⁵J. R. Ahn, H. W. Yeom, H. S. Yoon, and I.-W. Lyo, *Phys. Rev. Lett.* **91**, 196403 (2003).
⁶C. F. Hirjibehedin, C. P. Lutz, and A. J. Heinrich, *Science* **312**, 1021 (2006).
⁷J. N. Crain and D. T. Pierce, *Science* **307**, 703 (2005).
⁸N. Nilius, T. M. Wallis, and W. Ho, *Appl. Phys. A: Mater. Sci. Process.* **80**, 951 (2005).
⁹J. N. Crain, M. D. Stiles, J. A. Stroscio, and D. T. Pierce, *Phys. Rev. Lett.* **96**, 156801 (2006).
¹⁰P. Gambardella, H. Brune, K. Kern, and V. I. Marchenko, *Phys. Rev. B* **73**, 245425 (2006).
¹¹J. N. Crain and F. J. Himpsel, *Appl. Phys. A: Mater. Sci. Process.* **82**, 431 (2006).
¹²J. N. Crain, A. Kirakosian, K. N. Altmann, C. Bromberger, S. C. Erwin, J. L. McChesney, J.-L. Lin, and F. J. Himpsel, *Phys. Rev. Lett.* **90**, 176805 (2003); **92**, 089902(E) (2004).
¹³E. H. Lieb and F. Y. Wu, *Phys. Rev. Lett.* **20**, 1445 (1968).
¹⁴M. Ogata and H. Shiba, *Phys. Rev. B* **41**, 2326 (1990).
¹⁵H. Eskes, A. M. Oles, M. B. J. Meinders, and W. Stephan, *Phys. Rev. B* **50**, 17980 (1994).
¹⁶A. N. Kocharian, G. W. Fernando, K. Palandage, and J. W. Davenport, *Phys. Rev. B* **74**, 024511 (2006).
¹⁷G. Bedurftig, B. Brendel, H. Frahm, and R. M. Noack, *Phys. Rev. B* **58**, 10225 (1998).
¹⁸T. Giamarchi, *Quantum Physics in One Dimension* (Oxford Science, Oxford, 2004).
¹⁹H. Shiba and P. A. Pincus, *Phys. Rev. B* **5**, 1966 (1972).
²⁰C. A. Macedo and A. M. C. de Souza, *Phys. Rev. B* **65**, 153109 (2002).
²¹A. W. Sandvik, D. J. Scalapino, and C. Singh, *Phys. Rev. B* **48**, 2112 (1993); P. Sengupta, A. W. Sandvik, and D. K. Campbell, *ibid.* **65**, 155113 (2002).
²²Y. Wang, J. Voit, and Fu-Cho Pu, *Phys. Rev. B* **54**, 8491 (1996).
²³C. A. Stafford and A. J. Millis, *Phys. Rev. B* **48**, 1409 (1993).
²⁴Y. Umeno, M. Shiroishi, and A. Klümper, *Europhys. Lett.* **62**, 384 (2003).
²⁵B. Lazarovits, L. Szunyogh, and P. Weinberger, *Phys. Rev. B* **67**, 024415 (2003).
²⁶R. Preuss, A. Muramatsu, W. von der Linden, P. Dieterich, F. F. Assaad, and W. Hanke, *Phys. Rev. Lett.* **73**, 732 (1994).
²⁷H. Matsueda, N. Bulut, T. Tohyama, and S. Maekawa, *Phys. Rev. B* **72**, 075136 (2005).
²⁸Z.-Y. Lu, X.-G. Zhang, and S. T. Pantelides, *Phys. Rev. Lett.* **94**, 207210 (2005).
²⁹D. Rugar, H. J. Mamin, P. Guethner, S. E. Lambert, J. E. Stern, I. McFadyen, and T. Yogi, *J. Appl. Phys.* **68**, 1169 (1990).